

# Self-assembly of a peptide rod-coil: a polyproline rod and a cell-penetrating peptide Tat coil<sup>†</sup>

You-Rim Yoon, Yong-beom Lim, Eunji Lee and Myongsoo Lee\*

Received (in Cambridge, UK) 2nd January 2008, Accepted 22nd February 2008

First published as an Advance Article on the web 11th March 2008

DOI: 10.1039/b719868j

**Peptide rod-coil molecules, composed of a stiff polyproline rod and a hydrophilic cell-penetrating peptide Tat coil, self-assemble into nanocapsules and mediate efficient intracellular delivery of entrapped hydrophilic molecules.**

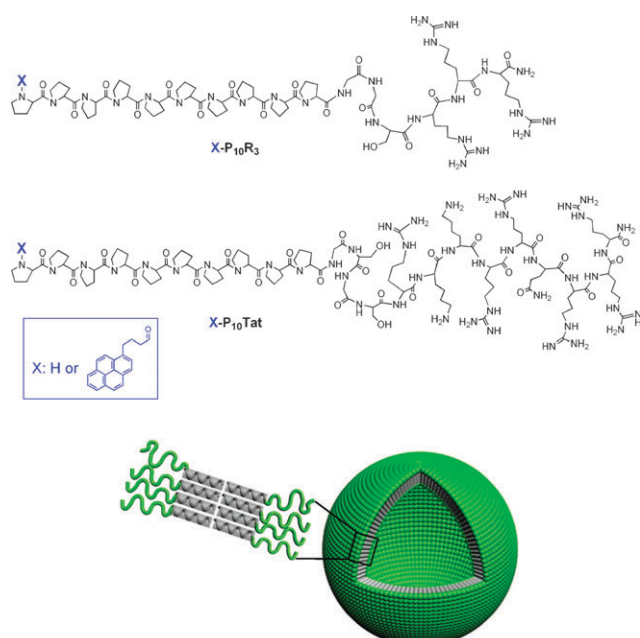
Rod-coil systems consisting of rigid hydrophobic rod and flexible hydrophilic coil segments are excellent building blocks for constructing well-defined supramolecular structures.<sup>1–5</sup> During the self-assembly process of rod-coil amphiphiles, the stiff and anisotropic ‘rod block’ has a tendency to impart orientational organization to supramolecular structures, while the flexible coil block can take on multiple shapes. In contrast to coil-coil block molecules, microphase separated supramolecular structures can generally form better in rod-coil block molecules even though the molecular weight of each block is very small, due to large chemical and stiffness differences between each block. Various types of supramolecular structures based on organic rod-coil building blocks have been constructed. In order to make use of these unique advantageous properties of rod-coil systems in creating biologically functional supramolecular structures, the rod-coil building blocks should be made of bioactive molecules.<sup>6–13</sup>

Herein, we report on the self-assembly of bioactive peptide rod-coils. In order to create the peptide rod, we have made use of a polyproline rod. Among the 20 naturally occurring amino acids, proline is the only one in which the side chain atoms form a pyrrolidine ring with the backbone atoms. As the cyclic structure of proline induces conformational constraints among the atoms in the pyrrolidine ring, the proline-rich sequences tend to form stiff helical rod structures, polyproline type II (PPII) helix, in aqueous solution.<sup>14–18</sup> The hydrophobicity of proline itself as an isolated amino acid is rather small. However, three nonpolar methylene groups are aligned at the outer part of the rod after PPII helix formation. Based on these facts, we hypothesized that stiff rod character and the nonpolar nature of outer surface of PPII helix might impart microphase separation characteristics to the rod-coil of a PPII rod and a hydrophilic coil, leading to the anisotropic orientational ordering of the rod and self-assembly.

As the biologically active and hydrophilic peptide coil, Tat cell penetrating peptide (CPP) was selected.<sup>19,20</sup> Tat CPP

(RKKRRQRRR) is a highly charged peptide with 8 positively charged residues (2 lysines and 6 arginines) and forms a random coil conformation in aqueous solution.<sup>7,8</sup> Tat CPP translocates into the inside of the cell efficiently. Many efforts have been made to utilize Tat CPP for delivering bioactive molecules, either by direct conjugation of the bioactive molecules with Tat CPP or by dendrimer and nanoparticle display of Tat CPP.<sup>19–21</sup> It has been shown that arginine residues in Tat CPP are primarily responsible for the cell binding and entry. Translocation efficiencies of arginine homo-oligomers, depending on the number of arginine residues, have been found to be comparable to or sometimes even better than that of wildtype Tat CPP.<sup>22,23</sup> With this in mind, we first synthesized a block peptide of a polyproline (10 prolines) and an arginine oligomer (3 arginines), P<sub>10</sub>R<sub>3</sub>, and investigated its self-assembly behavior (Scheme 1).

The secondary structure of P<sub>10</sub>R<sub>3</sub> in water investigated by circular dichroism (CD) spectroscopy shows that the spectrum is characteristic of a PPII helix<sup>18</sup> (Fig. 1a). In order to examine whether P<sub>10</sub>R<sub>3</sub> aggregates to form supramolecular nanostructures, a dynamic light scattering (DLS) experiment was performed (Fig. 1b). The result shows that P<sub>10</sub>R<sub>3</sub> aggregates well and forms nano-aggregates with a unimodal distribution of



**Scheme 1** Structures of peptide rod-coil building blocks and their self-assembly into nanocapsule structures.

Centre for Supramolecular Nano-Assembly, Department of Chemistry, Yonsei University, Shinchon 134, Seoul, 120-749, Korea. E-mail: mslee@yonsei.ac.kr; Fax: +82 2 393 6096; Tel: +82 2 2123 2647  
<sup>†</sup> Electronic supplementary information (ESI) available: Experimental procedures, MALDI-TOF MS spectra, light scattering data, TEM images, and CLSM images. See DOI: 10.1039/b719868j

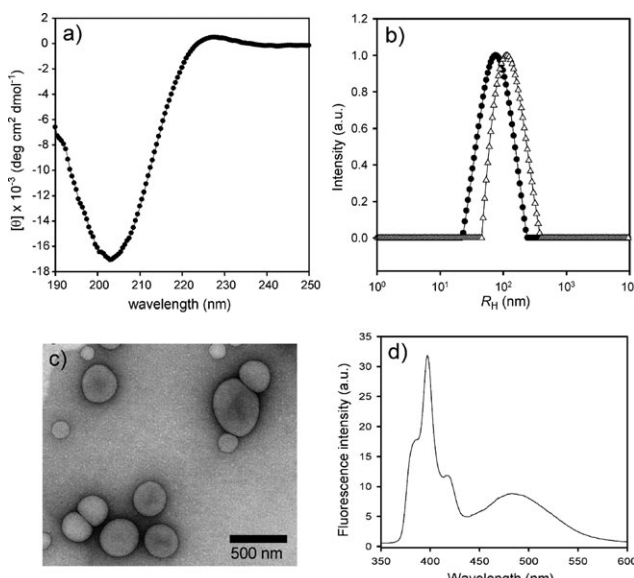


**Fig. 1** Self-assembly of peptide rod-coils. (a) CD spectrum of  $\text{P}_{10}\text{R}_3$  (100  $\mu\text{M}$ ) in water. (b) Distribution of  $R_{\text{H}}$  of  $\text{P}_{10}\text{R}_3$  aggregates (closed circles) and  $\text{P}_{10}\text{Tat}$  aggregates (open triangles) in water. (c) TEM image of  $\text{P}_{10}\text{R}_3$  aggregates in water. The sample was negatively stained with uranyl acetate. (d) Steady-state fluorescence emission spectra of pyr- $\text{P}_{10}\text{R}_3$  in water (300  $\mu\text{M}$ ).

hydrodynamic radius ( $R_{\text{H}}$ ). The average  $R_{\text{H}}$  of the aggregates was 74 nm. The nano-aggregates was confirmed to be spherical in shape, as revealed by transmission electron microscopy (TEM) examination (Fig. 1c). Considering the molecular length of  $\text{P}_{10}\text{R}_3$  (5.1 nm) with PPII rod (rise per residue,  $\sim 3.1 \text{ \AA}$ ) and extended peptide coil, the size of the spheres suggests that the objects are vesicles rather than micelles. In addition, the concaveness observed in the negatively stained TEM image indicates the shape of shrunken spheres formed during the drying process, providing further evidence of the hollow nature of the vesicular structures. These promising results prompted us to synthesize  $\text{P}_{10}\text{Tat}$ , which is likely to self-assemble into Tat CPP-coated vesicles. The studies show that  $\text{P}_{10}\text{Tat}$  forms a PPII helix and self-assembles into similar vesicular structures with average  $R_{\text{H}}$  of 115 nm (Fig. 1b). According to the classical theory of amphiphiles, an increase of the outer hydrophilic chain, while not changing the size of the hydrophobic chain, would increase the curvature of the amphiphile. This would then lead to a decreased aggregation number and therefore a decrease in amphiphile size. Contrary to the theory, the size increased from 74 nm to 115 nm (from  $\text{P}_{10}\text{R}_3$  to  $\text{P}_{10}\text{Tat}$ ) upon increasing the size of the hydrophilic chain. The classical theory best describes non-ionic amphiphiles. Therefore, it is likely that the self-assembly behavior of the highly charged hydrophilic segment might not follow the classical theory exactly. Moreover, the hydrogen bonding potential of guanidinium groups in arginines might make the description of the effects of the relative volume fractions of hydrophilic and hydrophobic segments on self-assembly even more complex.

To further investigate the aggregation behavior, we prepared pyr- $\text{P}_{10}\text{R}_3$  and pyr- $\text{P}_{10}\text{Tat}$  in which the fluorescent probe pyrenes were conjugated to the N-terminal parts of

$\text{P}_{10}\text{R}_3$  and  $\text{P}_{10}\text{Tat}$ , respectively. Both of the molecules were found to form a PPII helix and to self-assemble into vesicular structures. The average  $R_{\text{H}}$  of pyr- $\text{P}_{10}\text{R}_3$  and pyr- $\text{P}_{10}\text{Tat}$  vesicles were 141 nm and 127 nm, respectively. The steady-state fluorescence emission spectrum of pyr- $\text{P}_{10}\text{R}_3$  solution exhibits a large amount of excimer formation, indicating that pyrene molecules are located in close proximity due to self-assembly (Fig. 1d). The excimer started to form when the concentration of pyr- $\text{P}_{10}\text{R}_3$  reached 20  $\mu\text{M}$ . Fluorescence measurement revealed that pyr- $\text{P}_{10}\text{Tat}$  also formed excimers.

We next addressed the potential of the oligoarginine or Tat CPP-coated vesicles as carriers for delivering hydrophilic drug molecules into cells. As a model hydrophilic drug molecule, rhodamine B, a water-soluble fluorescent molecule, was used. For the entrapment, pyr- $\text{P}_{10}\text{R}_3$  (or pyr- $\text{P}_{10}\text{Tat}$ ) and rhodamine B were mixed together, sonicated, and the dye-loaded vesicles were separated from the free dye by using gel filtration chromatography. Successful entrapment of the dye was confirmed by fluorescence microscopic investigation of the separated vesicles (insets in Fig. 2a and b). The intracellular delivery experiment was performed in a mammalian cell line, HeLa. Intracellular fluorescence from the cells was observed by using confocal laser scanning microscopy (CLSM) after treatment of HeLa cells with the dye-loaded vesicles for 3 h (Fig. 2). The images in Fig. 2 show the cells treated with the dye-loaded pyr- $\text{P}_{10}\text{R}_3$  vesicles. The images reveal that the

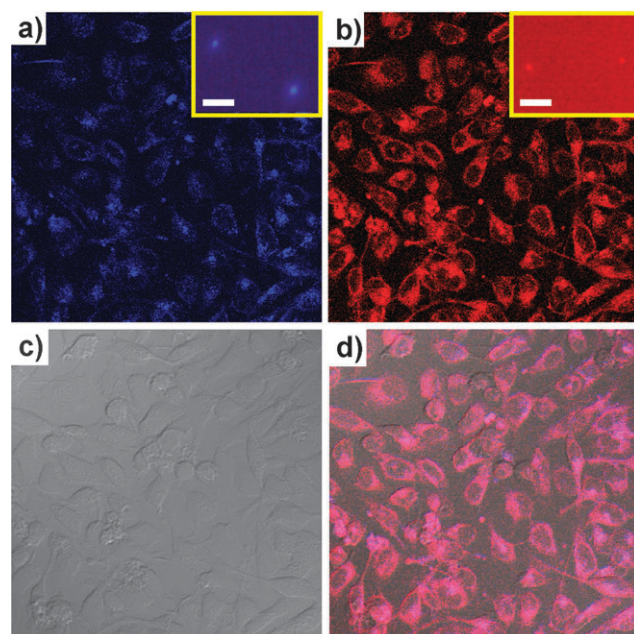


**Fig. 2** Intracellular delivery of hydrophilic dye-loaded pyr- $\text{P}_{10}\text{R}_3$  vesicles. CLSM image of HeLa cells after treating the cells with rhodamine B-loaded pyr- $\text{P}_{10}\text{R}_3$  vesicles for 3 h. (a) Intracellular fluorescence from pyr- $\text{P}_{10}\text{R}_3$ . Insets: Blue fluorescence of pyrene from rhodamine B-loaded pyr- $\text{P}_{10}\text{R}_3$  vesicles. Bar: 5  $\mu\text{m}$ . (b) Intracellular fluorescence from rhodamine B. Insets: Red fluorescence of rhodamine B from rhodamine B-loaded pyr- $\text{P}_{10}\text{R}_3$  vesicles. Bar: 5  $\mu\text{m}$ . (c) Bright field image of the cells. (d) Overlay of the blue and the red fluorescence images. The objects in the insets, although they are the same objects, are not in the same location between the figures because of their continuous Brownian motion.

pyr-P<sub>10</sub>R<sub>3</sub> vesicles and the entrapped dyes are efficiently delivered into the cells. The delivery experiment with the dye-loaded pyr-P<sub>10</sub>Tat vesicles resulted in similar efficient delivery and intracellular distribution pattern. Taken together, these results suggest that the oligomer of three arginines, a miniature of Tat CPP, is sufficient to promote efficient delivery of the vesicles. It is likely that the dense coating of arginines, although short, is responsible for the efficient delivery of pyr-P<sub>10</sub>R<sub>3</sub> vesicles and the entrapped cargos through multivalent effects.<sup>24</sup>

In summary, PPII rod–Tat CPP coil block peptides were prepared, and their self-assembly behavior and potential as intracellular delivery carriers were explored. In previous examples of self-assembly of peptide rod–coil molecules, a hydrophobic amino acid, such as leucine, was used as a rod building block.<sup>9,10</sup> This work emphasizes that the stiff rod character of the polyproline helix enables microphase separation of the slightly hydrophobic rod and the hydrophilic peptide coil, leading to the formation of self-assembled nanocapsules, which are stable enough to cross the cytoplasmic membrane barrier of the cell.

We gratefully acknowledge the National Creative Research Initiative Program of the Korean Ministry of Science and Technology for financial support of this work.

## Notes and references

- 1 M. Lee, B.-K. Cho and W.-C. Zin, *Chem. Rev.*, 2001, **101**, 3869.
- 2 W.-Y. Yang, J.-H. Ahn, Y.-S. Yoo, N.-K. Oh and M. Lee, *Nat. Mater.*, 2005, **4**, 399.
- 3 J.-H. Ryu, E. Lee, Y.-b. Lim and M. Lee, *J. Am. Chem. Soc.*, 2007, **129**, 4808.
- 4 H. M. König and A. F. M. Kilbinger, *Angew. Chem., Int. Ed.*, 2007, **46**, 8334.
- 5 B. W. Messmore, J. F. Hulvat, E. D. Sone and S. I. Stupp, *J. Am. Chem. Soc.*, 2004, **126**, 14452.
- 6 Y.-b. Lim and M. Lee, *Org. Biomol. Chem.*, 2007, **5**, 401.
- 7 Y.-b. Lim, E. Lee and M. Lee, *Angew. Chem., Int. Ed.*, 2007, **46**, 9011.
- 8 Y.-b. Lim, E. Lee and M. Lee, *Angew. Chem., Int. Ed.*, 2007, **46**, 3475.
- 9 E. P. Holowka, V. Z. Sun, D. T. Kamei and T. J. Deming, *Nat. Mater.*, 2007, **6**, 52.
- 10 E. P. Holowka, D. J. Pochan and T. J. Deming, *J. Am. Chem. Soc.*, 2005, **127**, 12423.
- 11 J. D. Hartgerink, E. Beniash and S. I. Stupp, *Science*, 2001, **294**, 1684.
- 12 S. Ghosh, M. Reches, E. Gazit and S. Verma, *Angew. Chem., Int. Ed.*, 2007, **46**, 2002.
- 13 A. Koide, A. Kishimura, K. Osada, W.-D. Jang, Y. Yamasaki and K. Kataoka, *J. Am. Chem. Soc.*, 2006, **128**, 5988.
- 14 S.-i. Sato, Y. Kwon, S. Kamisuki, N. Srivastava, Q. Mao, Y. Kawazoe and M. Uesugi, *J. Am. Chem. Soc.*, 2007, **129**, 873.
- 15 Y. A. Filon, J. P. Anderson and J. Chmielewski, *J. Am. Chem. Soc.*, 2005, **127**, 11798.
- 16 B. Schuler, E. A. Lipman, P. J. Steinbach, M. Kumke and W. A. Eaton, *Proc. Natl. Acad. Sci. U. S. A.*, 2005, **102**, 2754.
- 17 M. Kumin, L.-S. Sonntag and H. Wennemers, *J. Am. Chem. Soc.*, 2007, **129**, 466.
- 18 L. Crespo, G. Sanclimens, B. Montaner, R. Perez-Tomas, M. Royo, M. Pons, F. Albericio and E. Giralt, *J. Am. Chem. Soc.*, 2002, **124**, 8876.
- 19 S. Futaki, *Adv. Drug Delivery Rev.*, 2005, **57**, 547.
- 20 V. P. Torchilin, R. Rammohan, V. Weissig and T. S. Levchenko, *Proc. Natl. Acad. Sci. U. S. A.*, 2001, **98**, 8786.
- 21 S. R. Schwarze, A. Ho, A. Vocero-Akbani and S. F. Dowdy, *Science*, 1999, **285**, 1569.
- 22 P. A. Wender, D. J. Mitchell, K. Pattabiraman, E. T. Pelkey, L. Steinman and J. B. Rothbard, *Proc. Natl. Acad. Sci. U. S. A.*, 2000, **97**, 13003.
- 23 S. Futaki, T. Suzuki, W. Ohashi, T. Yagami, S. Tanaka, K. Ueda and Y. Sugiura, *J. Biol. Chem.*, 2001, **276**, 5836.
- 24 M. Sung, G. M. K. Poon and J. Gariépy, *Biochim. Biophys. Acta Biomembr.*, 2006, **1758**, 355.